Corrosion of Carbon Steel in MDEA-Based CO_2 Capture Plants Under Regenerator Conditions: Effects of O_2 and Heat-Stable Salts

Yong Xiang, Yoon-Seok Choi,‡,* Yang Yang,* and Srdjan Nešić**

ABSTRACT

The corrosion behavior of carbon steel UNS K02600 in 50 wt% methyldiethanolamine solutions was investigated in the background of the carbon dioxide (CO_2) capture process in fossil fuel-fired power plants for the purpose of carbon capture and storage. A series of experiments was conducted under regenerator conditions (120°C) with different combinations of CO_2 loading (0.3 mol/mol and 0.05 mol/mol), O_2, and heat-stable salts (including sulfate, formate, and N,N-bis[2-hydroxyethyl] glycine). The corrosion behavior of carbon steel was investigated using electrochemical techniques (open circuit potential, linear polarization resistance, and potentiodynamic polarization), surface analytical techniques (scanning electron microscopy, energy-dispersive x-ray spectroscopy, and x-ray diffraction), and weight-loss methods. The results showed that the corrosion rate of carbon steel initially decreased and then stabilized with time in CO_2-loaded methyldiethanolamine solution due to the formation of an iron carbonate ($FeCO_3$) layer, with the exception of methyldiethanolamine/CO_2/O_2/heat-stable salts, which exhibited a low CO_2 loading (0.05 mol/mol). It was found that the presence of HSS significantly accelerated the corrosion process at low CO_2 loading, whereas the effect of oxygen on the corrosion rate was not significant at low CO_2 loading. The formation mechanism of the $FeCO_3$ layer, which is a key issue in the control of corrosion in these environments, was discussed.

KEY WORDS: carbon dioxide capture, carbon dioxide corrosion, iron carbonate, heat-stable salts, methyldiethanolamine, O_2, regenerator

INTRODUCTION

Alkanolamine-based solutions are widely used in the petroleum and natural gas industries to remove undesirable gases, particularly two acid gases: hydrogen sulfide (H_2S) and carbon dioxide (CO_2).[1] When alkanolamine-based solutions are applied to deal with the flue gas from coal-fired power plants for the purpose of carbon capture and storage (CCS), the corrosion mechanism of steel in these environments might be changed by the presence of impurity gases such as SO_x, NO_x, and O_2, which are not usually contained in the natural gas purification process. When O_2 exists, it may participate in the cathodic reactions and contribute to the degradation of alkanolamine.[2] When acid gas impurities as SO_x and NO_x are involved in the capture process, heat-stable salts (HSS) could easily form from the degradation process of alkanolamine, especially when associated with O_2. The effects of O_2, NO_x, and SO_x on the alkanolamine system have not been thoroughly evaluated, although some studies have addressed this issue.[3-4]

Methyldiethanolamine (MDEA) is considered to be a less-corrosive amine than monoethanolamine (MEA) and diethanolamine (DEA).[5] Unlike for MEA, no carbamate (NH_2COOH) is formed when MDEA absorbs CO_2. When the CO_2 flows into the capture unit, the following reactions occur:[6-7]

Submitted for publication: May 23, 2014. Revised and accepted: August 6, 2014. Preprint available online: September 3, 2014, doi: http://dx.doi.org/10.5006/1354.

‡ Corresponding author. E-mail: choiy@ohio.edu.

* Institute for Corrosion and Multiphase Technology, Department of Chemical and Biomolecular Engineering, Ohio University, 342 West State Street, Athens, OH 45701.

ISSN 0010-9312 (print), 1938-159X (online)
15/0000005/$5.00+$0.50/0

In absorber (Equation [1]):

$$R_3N + CO_2 + H_2O \rightarrow R_3NH^+ + HCO_3^- \quad (1)$$

In regenerator (Equation [2]):

$$R_3NH^+ + HCO_3^- + \text{heat} \rightarrow R_3N + CO_2 + H_2O \quad (2)$$

Some papers have reported on steel corrosion in MDEA solution.[8-15] Rooney, et al., compared the corrosivities of different HSS in MDEA solution.[12-13] Guo and Tomoe studied the effects of corrosion product layers on anodic dissolution and cathodic reduction in CO_2-loaded MDEA solutions using impedance, potentiodynamic polarization techniques, and x-ray diffraction (XRD).[15] Although the effects of O_2 and HSS on the corrosion behavior of carbon steel in CO_2-loaded MDEA solutions under absorber conditions have been studied thoroughly,[8] their effects under regenerator conditions still require further investigation. Regenerator conditions are characterized by a higher operation pressure and temperature (usually around 120°C).[16] For typical CO_2 corrosion, the formation of an iron carbonate ($FeCO_3$) layer under high-temperature conditions is favorable,[17-19] which can drastically depress the corrosion rate.[18,20]

The objective of the present study was to investigate the effects of O_2 and HSS on the corrosion behavior of carbon steel UNS K02600[(1)] in CO_2-loaded MDEA solution under regenerator conditions related to the CO_2 capture process in coal-fired power plants, especially to monitor the variations in corrosion rate with time. Carbon steel was selected because it is widely used in regenerator shells and easily develops corrosion problems. Sulfate, formate, and N,N-bis (2-hydroxyethyl) glycine (bicine) were selected as HSS for the current study. Sulfate is supposed to be the reaction product of SO_2, O_2, and alkanolamine.[3] Formate is a common degradation product of the MDEA system.[21-22] Bicine can form in a MDEA solution when subjected to O_2 contamination.[2,23] The most likely way to form bicine involves the disproportionation reaction of MDEA to triethanolamine (TEA) and other mixed amines followed by the further oxidation of TEA to bicine.[24] Bicine is thought to contribute to the corrosiveness of gas-treating amine solutions,[25] as evidenced by autoclave tests.[23] Deprotonated bicine can react with Fe^{2+}, acting as a strong chelator (Equations [3] and [4]):[26]

$$Fe^{2+} + \text{bicine}^{-1} \underset{}{\overset{K_{ML}=10^{4.3}}{\rightleftharpoons}} [Fe(\text{bicine})]^+ \quad (3)$$

$$[Fe(\text{bicine})]^+ + \text{bicine}^{-1} \underset{}{\overset{K_{ML2}=10^{3.0}}{\rightleftharpoons}} [Fe(\text{bicine})_2] \quad (4)$$

where K_{ML} and K_{ML2} are the equilibrium constants in Equations (3) and (4), respectively.

EXPERIMENTAL PROCEDURES

An aqueous solution with a concentration of 50% MDEA by weight was prepared from a 99% MDEA reagent and deionized water. The sample material was carbon steel UNS K02600, which has the following chemical composition: 0.23% C, 0.79% Mn, 0.02% P, 0.03% S, 0.29% Cu, 0.20% Si, and balance Fe. The samples were progressively polished with silicon carbide (SiC) paper up to 600 grit, washed by isopropyl alcohol (C_3H_8O) in an ultrasonic bath, and finally dried. The total concentration of HSS was about 15,800 ppmw (3,002 ppmw sulfuric acid [H_2SO_4] + 2,818 ppmw formic acid [CH_2O_2] + 10,000 ppmw bicine); the HSS were added by dissolving their acid forms in the MDEA solution.

Figure 1 shows the schematic of the experimental setup. All the tests were carried out in an autoclave at 120°C. The total pressure of each test depended on the CO_2 and O_2 partial pressures and included the saturated water vapor pressure at 120°C.

The test matrix for the current study is shown in Table 1. Different combinations of test parameters were used to investigate the effects of O_2 and HSS. The desired CO_2 loading (0.05 mol/mol and 0.3 mol/mol) was obtained by controlling the CO_2 partial pressure for each test.[9] With 8 psi (55 kPa) of O_2 partial pressure, the concentration of dissolved O_2 in the MDEA solution was around 14 ppmw,[27] considering that the solubility of O_2 in MDEA solution is close to that in water.[28]

The corrosion behavior of carbon steel was investigated by electrochemical techniques including linear polarization resistance (LPR), open-circuit potential (OCP), and potentiodynamic polarization measurements. The weight-loss method was also used to measure the corrosion rate. Scanning electron microscopy (SEM) was used to observe the surface morphology,

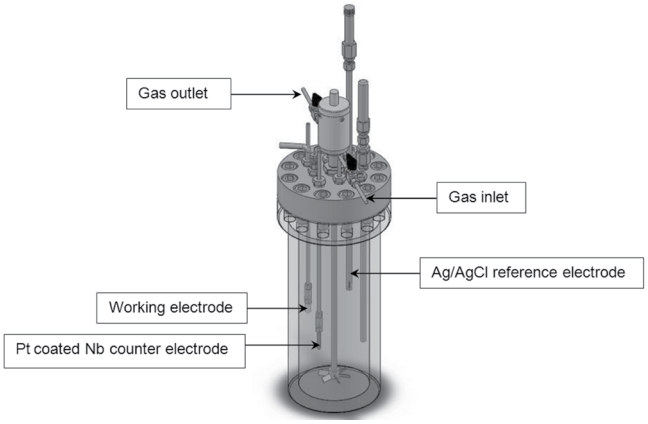

FIGURE 1. *Schematic of autoclave system equipped for electrochemical measurements.*

(1) UNS numbers are listed in *Metals and Alloys in the Unified Numbering System*, published by the Society of Automotive Engineers (SAE International) and cosponsored by ASTM International.

TABLE 1
Test Matrix for Corrosion Testing at Regenerator Conditions

Test No.	CO_2 Loading (mol/mol)	CO_2 Partial Pressure (psi [kPa])	O_2 Partial Pressure (psi [kPa])	Total Pressure (psi [kPa])	HSS
1	0.05	7 (48)	0 (0)	36 (248)	No
2	0.05	7 (48)	8 (55)	44 (303)	No
3	0.05	7 (48)	8 (55)	44 (303)	Yes
4	0.3	148 (1,020)	0 (0)	177 (1,220)	No
5	0.3	148 (1,020)	0 (0)	177 (1,220)	Yes
6	0.3	148 (1,020)	8 (55)	185 (1,276)	Yes

while energy-dispersive x-ray spectroscopy (EDS) and XRD were used to detect the element and phase compositions of the corrosion products, respectively.

Figure 2 illustrates the experimental procedures. First, a 50-wt% MDEA solution was poured into the autoclave, and the solution was purged with CO_2 for several hours depending on the desired CO_2 loading for each experiment. Subsequently, the specimens were installed in the autoclave. After the autoclave was sealed, it was heated to 120°C, and the total pressure was adjusted by venting the autoclave. Oxygen was then added to the desired partial pressure if needed in the test.

RESULTS AND DISCUSSION

Effects of O_2 and Heat-Stable Salts Under the High-CO_2-Loading Condition (0.3 mol/mol)

Figure 3 shows the variations in OCP and corrosion rate with time for carbon steel UNS K02600 in CO_2-loaded MDEA solutions under different O_2 and HSS conditions at a CO_2 loading of 0.3 mol/mol. The OCP values initially increased with time and eventually reached stable values, especially for the MDEA/CO_2/HSS and MDEA/CO_2/O_2/HSS solutions. Meanwhile, the OCP values of the MDEA/CO_2/HSS and MDEA/CO_2/O_2/HSS solutions had lower initial values than the MDEA/CO_2 solution. As shown in Figure 3(b), the addition of O_2 or HSS increased the corrosion rate at the initial stage, but the corrosion rates sharply decreased to relatively low values (less than 0.01 mm/y) in the first 10 h for all conditions, which might be related to the inhibition effect of the corrosion product layers.

Figure 4 shows the polarization curves of carbon steel UNS K02600 in CO_2-loaded MDEA solutions (0.3 mol/mol) under different conditions after 48 h of exposure. This figure indicates that the corrosion potential values were similar for the three cases at the end of the tests, and the final corrosion rates all seem to be low. The anodic curves revealed that no obvious passive zones were observed in all cases, especially for the MDEA/CO_2/HSS solution, whose current density increased monotonically with potential.

Table 2 shows the corrosion rates obtained from weight-loss measurements for different O_2 and HSS

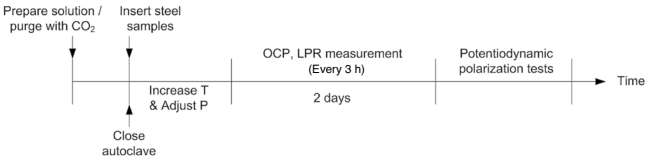

FIGURE 2. *Experimental procedure for corrosion testing under regenerator conditions.*

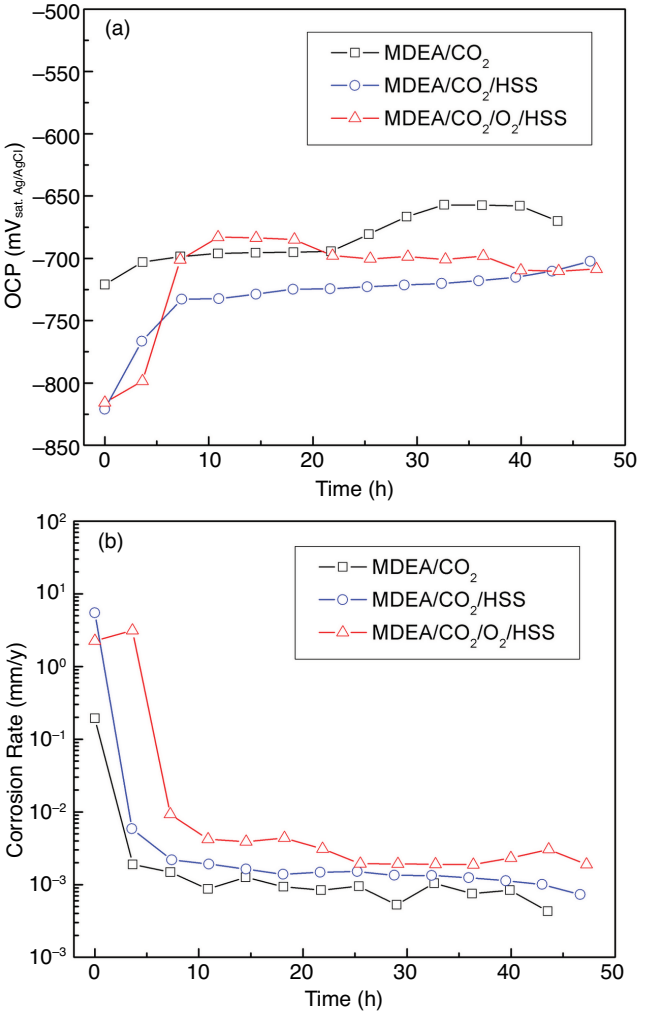

FIGURE 3. *Variations in OCP and corrosion rate with time of carbon steel UNS K02600 in CO_2-loaded MDEA solutions (0.3 mol/mol) under different O_2 and HSS conditions: (a) OCP and (b) corrosion rate (B = 13 mV/decade).*

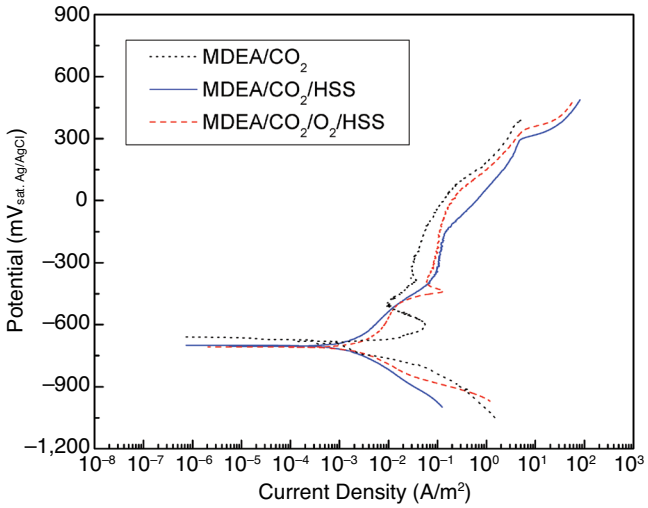

FIGURE 4. *Potentiodynamic curves of carbon steel UNS K02600 in CO_2-loaded MDEA solution (0.3 mol/mol) after 48 h of exposure.*

conditions in CO_2-loaded MDEA solutions (0.3 mol/mol). The solution with both O_2 and HSS had the highest corrosion rate, while the case without O_2 and HSS had the lowest corrosion rate. The corrosion rates determined from weight-loss measurements shown in Table 2 confirmed that the addition of O_2 or HSS increased the corrosion rate under the high CO_2-loading condition; however, the weight-loss corrosion rate is a time-averaged value that does not provide information about time-specific corrosion rates when the corrosion rate changes with time.

The SEM images and EDS spectra of the corroded sample surfaces of carbon steel UNS K02600 in CO_2-loaded MDEA solutions for the high CO_2-loading (0.3 mol/mol) are shown in Figure 5. It is obvious that some corrosion products accumulated on the sample surfaces, and they compactly covered the entire sample surface in all cases. The EDS analysis indicated the existence of Fe, C, and O elements, which might suggest the formation of $FeCO_3$ layers.

The XRD spectra of the corrosion products of carbon steel UNS K02600 in CO_2-loaded MDEA solutions at the high CO_2-loading condition are illustrated in Figure 6. The XRD spectra verified that the corrosion product was $FeCO_3$ in all cases, and no other crystalline product was detected by XRD. This result provided an explanation for the decrease in corrosion rate with time. It seems likely that the additions of O_2 and HSS did not interrupt the formation of protective $FeCO_3$ under the high CO_2-loading condition.

The above results indicate that for the MDEA-based CO_2 capture plant, the corrosion risk is decreased by the formation of the $FeCO_3$ layer under regenerator conditions (120°C). If the $FeCO_3$ layer can be maintained integrally in the daily operation, the use of carbon steel as one of the manufacturing materials for the parts that work under high CO_2-loading conditions in the regenerator might be acceptable considering the corrosion protection effect of the $FeCO_3$ layer.

In general, however, the CO_2 loading in most parts of the regenerator is low because CO_2 escapes

TABLE 2

Weight-Loss Corrosion Rates for Different O_2 and Heat-Stable Salt Conditions of Carbon Steel UNS K02600 in CO_2-Loaded MDEA Solutions (0.3 mol/mol)

Condition	MDEA/CO_2	MDEA/CO_2/HSS	MDEA/CO_2/O_2/HSS
Corrosion rate (mm/y)	0.13±0.02	0.32±0.05	0.75±0.06

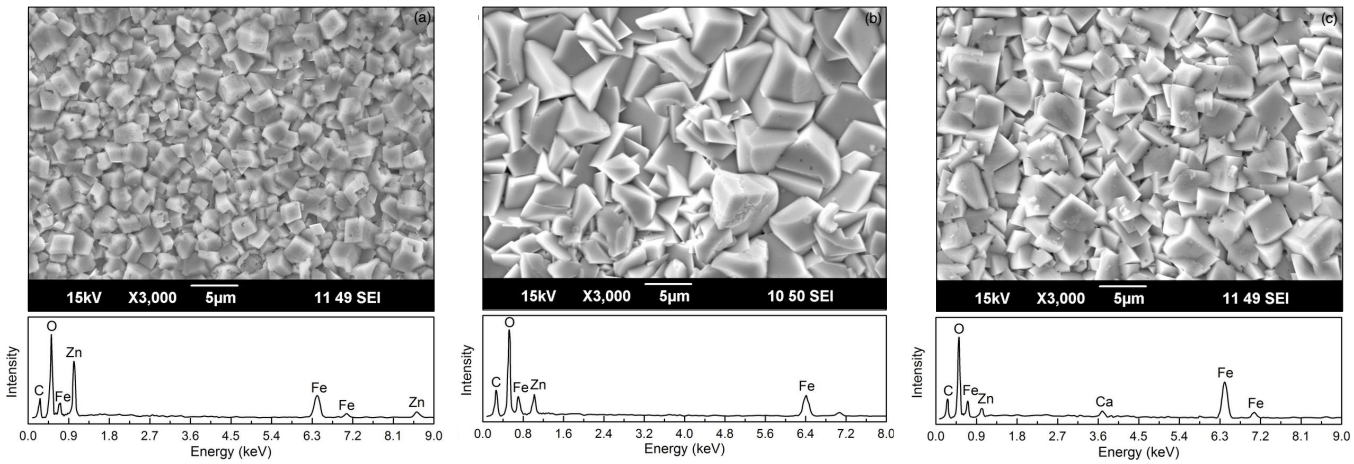

FIGURE 5. *SEM images and EDS spectra of the corroded sample surfaces of carbon steel UNS K02600 in CO_2-loaded MDEA solutions (0.3 mol/mol): (a) MDEA/CO_2; (b) MDEA/CO_2/HSS; and (c) MDEA/CO_2/O_2/HSS.*

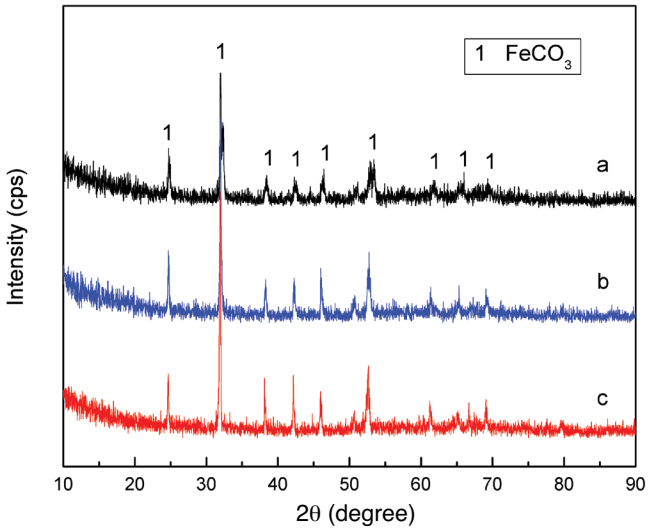

FIGURE 6. *XRD spectra of corrosion products of carbon steel UNS K02600 in CO_2-loaded MDEA solutions (0.3 mol/mol): (a) MDEA/CO_2; (b) MDEA/CO_2/HSS; and (c) MDEA/CO_2/O_2/HSS.*

from solution at high temperature. Therefore, the next section discusses the tests under the low CO_2-loading condition.

Effect of O_2 and Heat-Stable Salts Under the Low CO_2-Loading Condition (0.05 mol/mol)

The variations in the OCP and corrosion rate of carbon steel UNS K02600 in CO_2-loaded MDEA solutions (0.05 mol/mol) are shown in Figure 7. For the MDEA/CO_2 and MDEA/CO_2/O_2 solutions, the OCP value increased in the first 20 h, while for the MDEA/CO_2/O_2/HSS solution, the OCP value remained at a stable value close to the initial potential. For MDEA/CO_2/O_2/HSS, the corrosion rate of carbon steel remained at a relative higher value compared to the other solutions under low CO_2 loading. Actually, the corrosion rate increased slightly with time from 1.65 mm/y to 2.05 mm/y for the MDEA/CO_2/O_2/HSS solution under 0.05 mol/mol CO_2 loading. This indicates that the addition of HSS significantly accelerated the corrosion rate, while the acceleration effect of O_2 was limited; with the addition of O_2, the corrosion rate eventually decreased to a low value, but the duration of the period of high corrosion rate was longer than that for MDEA/CO_2.

The polarization curves under the low CO_2-loading condition are shown in Figure 8. The solution with both O_2 and HSS had the highest corrosion rate and the most negative OCP value at the end of the test. Its anodic part seemed to show passive behavior, although the passive current density was much higher than for the other solutions. However, for the MDEA/CO_2 and MDEA/CO_2/O_2 solutions, the corrosion rates seemed to be relatively low at the end of the tests, and they did not show the obvious passive regions. Therefore, it seems that the effect of HSS on the corrosion

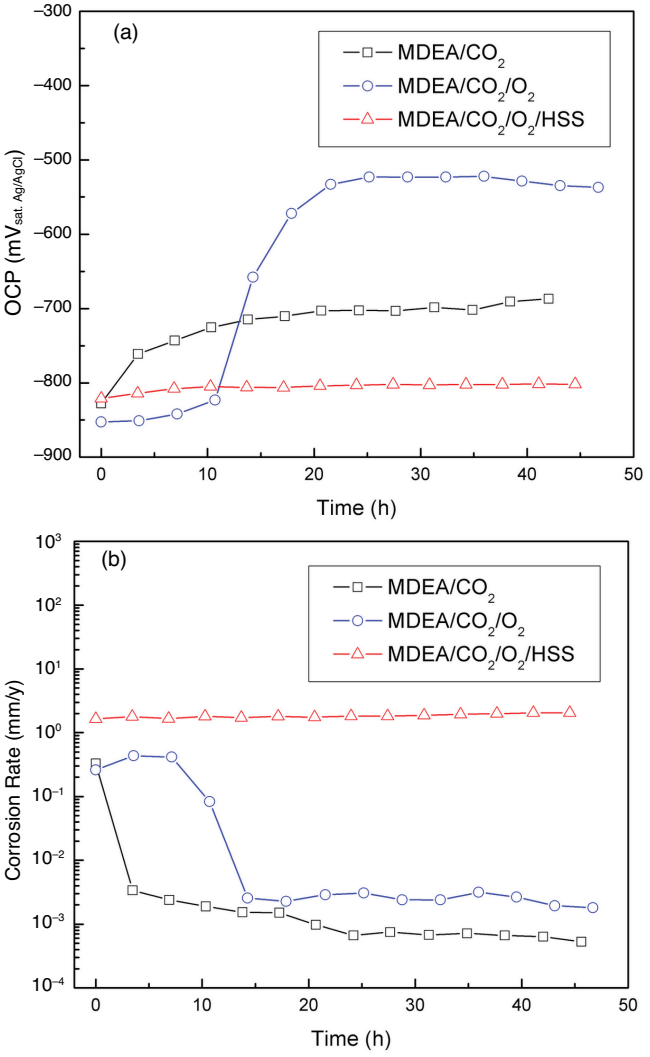

FIGURE 7. *Variations in OCP and corrosion rate with time of carbon steel UNS K02600 in CO_2-loaded MDEA solutions (0.05 mol/mol) under different O_2 and HSS conditions: (a) OCP and (b) corrosion rate (B = 13 mV/decade).*

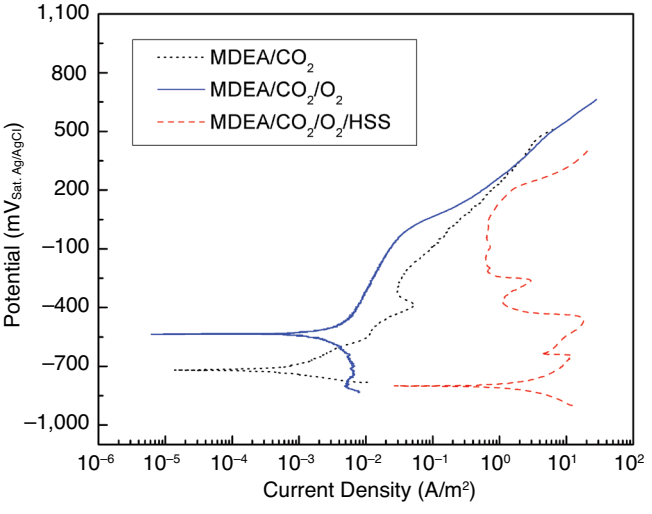

FIGURE 8. *Potentiodynamic curves of carbon steel UNS K02600 in CO_2-loaded MDEA solution (0.05 mol/mol) after 48 h of exposure.*

rate was more significant than that of O_2 under the low CO_2-loading condition.

The results of the weight-loss measurements for the low CO_2-loading condition (0.05 mol/mol) are shown in Table 3, which shows that the results are similar to the results of the LPR measurements and potentiodynamic sweeps. The MDEA/CO_2/O_2/HSS solution had the highest corrosion rate, while the corrosion rates for the MDEA/CO_2 and MDEA/CO_2/O_2 solutions were both low. This result confirmed that the effect of HSS on the corrosion rate was obvious under this low CO_2-loading condition, which can possibly increase the corrosion rate by interrupting the formation of the protective $FeCO_3$ layer. The average corrosion rate obtained from the LPR method is 1.84 mm/y for the MDEA/CO_2/O_2/HSS solution (0.05 mol/mol), which is the same as the corrosion rate obtained by the weight-loss method; this indicates that the B value (13 mV/decade) used in the current work is reasonable.

Figure 9 shows the SEM images and EDS spectra of the corroded sample surfaces of carbon steel UNS K02600 in CO_2-loaded MDEA solutions (0.05 mol/mol). It was found that the continuous $FeCO_3$ layer was formed for the MDEA/CO_2 and MDEA/CO_2/O_2 solutions, but not for MDEA/CO_2/O_2/HSS. For this last solution, three typical areas were scanned by EDS, as shown in Figure 9(c). Area I should correspond to Fe_3C,[8,29] Area II might be the small $FeCO_3$ precipitation particles, and Area III should be the ferrite substrate.[8] It seems that the addition of HSS can inhibit the formation of the protective $FeCO_3$ layer at the low CO_2-loading (0.05 mol/mol), though the mechanism requires a more thorough analysis.

The controlling factor for the precipitation of $FeCO_3$ is the saturation degree (SD) of $FeCO_3$ (Equation [5]):

$$SD = \frac{[Fe^{2+}][CO_3^{2-}]}{K_{sp}} \quad (5)$$

where K_{sp} is the solubility constant of $FeCO_3$ in mol^2/L^2, $[CO_3^{2-}]$ is the concentration of the carbonate ion in mol/L, and $[Fe^{2+}]$ is the concentration of ferrous ion

TABLE 3

Weight-Loss Corrosion Rates for Different O_2 and Heat-Stable Salt Conditions of Carbon Steel UNS K02600 in CO_2-Loaded MDEA Solutions (0.05 mol/mol)

Condition	MDEA/CO_2	MDEA/CO_2/O_2	MDEA/CO_2/O_2/HSS
Corrosion rate (mm/y)	0.14±0.02	0.14±0.02	1.84±0.05

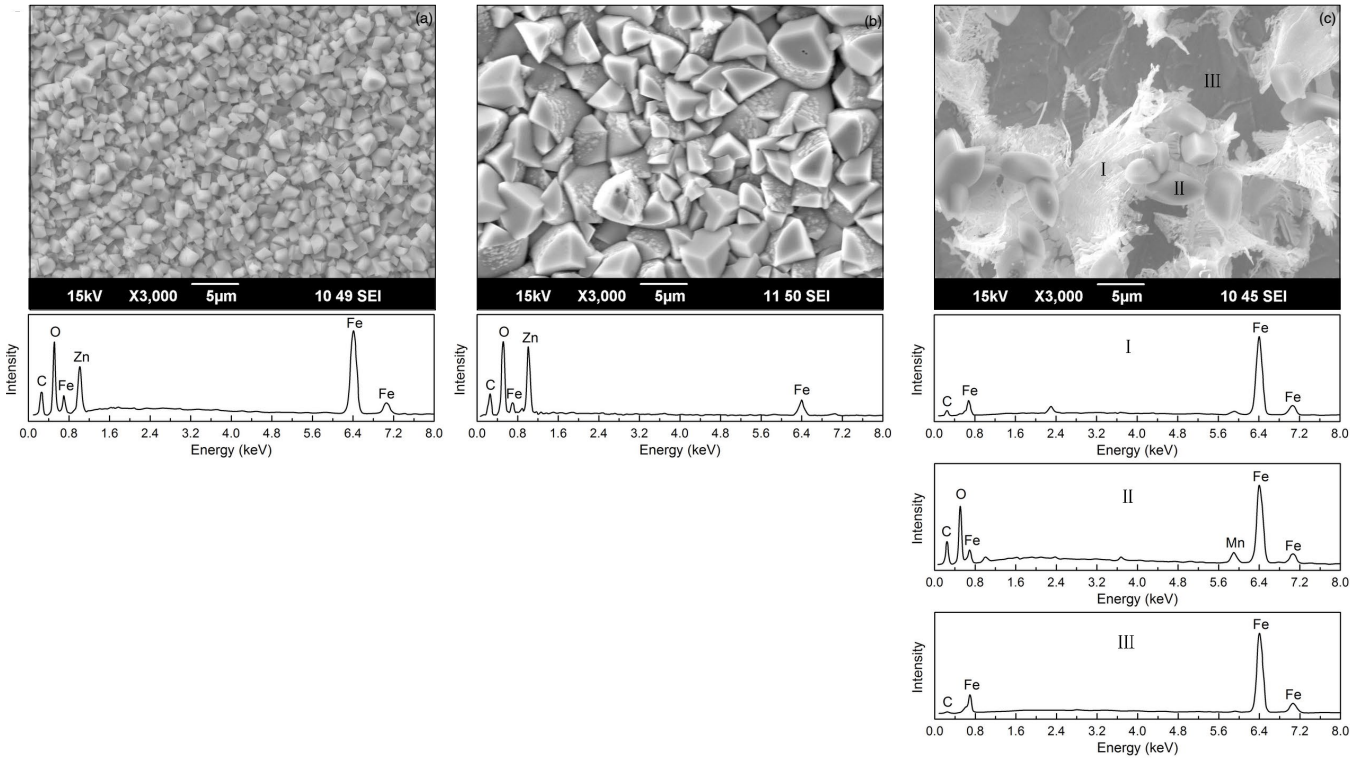

FIGURE 9. *SEM images and EDS spectra of the corroded sample surfaces of carbon steel UNS K02600 in CO_2-loaded MDEA solutions (0.05 mol/mol): (a) MDEA/CO_2; (b) MDEA/CO_2/O_2; and (c) MDEA/CO_2/O_2/HSS.*

TABLE 4
Comparison of SD, K_{sp}, Fe^{2+}, and CO_3^{2-} Values Under Different Conditions

Condition	CO_3^{2-}	Fe^{2+}	K_{sp}	SD
0.05 mol/mol, CO_2	Low	—	—	>1
0.05 mol/mol, CO_2/O_2	Low	—	—	>1
0.05 mol/mol, CO_2/O_2/HSS	Low	Decreased[(A)]	Increased[(B)]	<1
0.3 mol/mol, CO_2	High	—	—	>1
0.3 mol/mol, CO_2/HSS	High	Decreased[(A)]	Increased[(B)]	>1
0.3 mol/mol, CO_2/O_2/HSS	High	Decreased[(A)]	Increased[(B)]	>1

[(A)] Decreased by chelating effect of bicine.
[(B)] Increased by HSS (by increasing ionic strength).

in mol/L. $FeCO_3$ will precipitate when the SD value exceeds unity, i.e., when the solution is supersaturated.

When the CO_2 loading is high, the concentration of CO_3^{2-} and the SD value should be high, making it easier to form the $FeCO_3$ layer. Based on the current test results, there is a possibility that the addition of HSS increases the solubility of $FeCO_3$ in the MDEA solution, which reduces the SD value of $FeCO_3$ in the MDEA solution, especially at the low CO_2-loading condition. The presence of HSS may affect the SD value in the following ways:

—The chelating effect of bicine on free Fe^{2+} ions seems to contribute to the reduction of the SD value of $FeCO_3$ when HSS are added.
—The addition of HSS (acid forms) may result in a lower pH and eventually lead to a lower CO_3^{2-} concentration.
—The addition of HSS may increase the K_{sp} value by increasing the ionic strength.

It is well known that the $FeCO_3$ solubility is increased by reducing the temperature.[30-31] Actually, the solubility constant, K_{sp}, of $FeCO_3$ is a function of both ionic strength and temperature.[32] The expression proposed by Sun, et al.,[32] provides an accurate prediction compared with the experimental data for both changing temperature and ionic strength (Equation [6]):

$$\log K_{sp} = -59.3498 - 0.041377T_k - \frac{2.1963}{T_k} + 24.5724\log(T_k) + 2.518I^{0.5} - 0.657I \quad (6)$$

Both the related experimental data[33] and Equation (6) show that when the ionic strength is less than about 4 mol/L, the K_{sp} of $FeCO_3$ increases with increasing ionic strength, and the effect is more significant when the ionic strength is low. The addition of HSS (in acid form) increased ionic strength by introducing the following reaction with the CO_2-free alkanolamine molecules Equation [7]:

$$\text{Alkanolamine} + \text{Acid} \rightarrow \text{Salt} \quad (7)$$

Table 4 clearly shows how the SD values are affected by different kinds of factors. Through this analysis, it is clear why the MDEA/CO_2/O_2/HSS (0.05 mol/mol) solution did not form the continuous $FeCO_3$ precipitation layer and therefore had the highest corrosion rate.

The comparison of the LPR corrosion rates over time for the high and low CO_2-loading conditions is shown in Figure 10. Although a lower CO_2 loading of the alkanolamine solution always results in a lower steel corrosion rate,[34-36] the results of the current study showed that when O_2 and HSS were present, the corrosion rate under the 0.05 mol/mol CO_2-loading condition was higher than that under the 0.3 mol/mol condition as a result of the lack of corrosion inhibition effect of the $FeCO_3$ layer, which always formed under the high CO_2-loading condition. Therefore, when applied for CCS purposes where O_2 and HSS are inevitably contained in the MDEA solution, the corrosion risk of the carbon steel is much higher under low CO_2-loading conditions than under high CO_2-loading conditions in the regenerator. Stainless steel might be used as the construction material for the parts of the regenerator that work under low CO_2-loading conditions; in other cases, the use of corrosion inhibitors might be needed. By the skilled application of ion exchange, the HSS-like bicine can also be removed and maintained at very low levels that will reduce or prevent corrosion.[37]

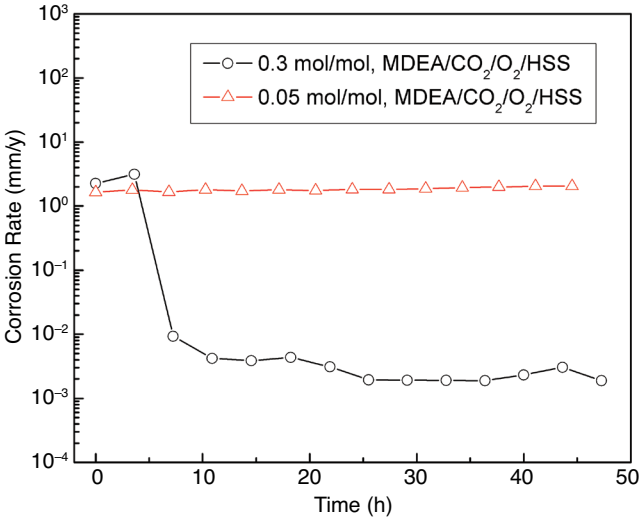

FIGURE 10. *Comparison of LPR corrosion rates under high and low CO_2 loading conditions (B = 13 mV/decade).*

CONCLUSIONS

The current study investigated the effects of O_2 and HSS on the corrosion behavior of carbon steel UNS K02600 in MDEA solutions under both high and low CO_2-loading conditions. The following findings and conclusions were obtained:

❖ Both O_2 and HSS increased the corrosion rate of carbon steel UNS K02600 in CO_2-loaded MDEA solutions, mainly at the initial stage.

❖ The corrosion rate of carbon steel UNS K02600 decreased at the initial stage because of the formation of an $FeCO_3$ layer, except for in the solution containing both O_2 and HSS under the low CO_2-loading condition (0.05 mol/mol).

❖ The MDEA/CO_2/O_2/HSS solution had a higher average corrosion rate under the low CO_2-loading condition (0.05 mol/mol) than under the high CO_2-loading condition (0.3 mol/mol) because the inhibition effect of the continuous $FeCO_3$-layer on the underlying steel was absent under the low CO_2-loading condition.

ACKNOWLEDGMENTS

The authors would like to acknowledge the financial support from Alstom Power Inc. for the Institute for Corrosion and Multiphase Technology at Ohio University. The authors also would like to thank D. Wang for executing the XRD tests.

REFERENCES

1. J. Kittel, E. Fleury, B. Vuillemin, S. Gonzalez, F. Ropital, R. Oltra, *Mater. Corros.-Werkst. Korros.* 63, 3 (2012): p. 223-230.
2. J.E. Critchfield, J.L. Jenkins, *Petrol. Technol. Quarterly* Spring (1999): p. 87-95.
3. S. Zhou, S. Wang, C. Chen, *Ind. Eng. Chem. Res.* 51, 6 (2012): p. 2539-2547.
4. P. Wattanaphan, T. Sema, R. Idem, Z. Liang, P. Tontiwachwuthikul, *Int. J. Greenhouse Gas Control* 19 (2013): p. 340–349.
5. M.S. Dupart, T.R. Bacon, D.J. Edwards, *Hydrocarbon Processing* 72, 5 (1993): p. 89-94.
6. A.L. Cummings, G.D. Smith, D.K. Nelsen, *Advances in Amine Reclaiming—Why There's No Excuse to Operate a Dirty Amine System* (Norman, OK: University of Oklahoma OUTREACH, 2007) p. 227.
7. R.B. Nielsen, K.R. Lewis, J.G. McCullough, D.A. Hansen, *Controlling Corrosion in Amine Treating Plants* (Norman, OK: University of Oklahoma OUTREACH, 1995) p. 182.
8. Y.S. Choi, D. Duan, S. Nešić, F. Vitse, S.A. Bedell, C. Worley, *Corrosion* 66, 12 (2010): p. 125004.
9. Y.-S. Choi, S. Nešić, D. Duan, S. Jiang, *Corrosion* 69, 6 (2013): p. 551-559.
10. D. Duan, Y.-S. Choi, S. Jiang, S. Nešić, "Corrosion Mechanism of Carbon Steel in MEA-Based CO_2 Capture Plants," CORROSION/2013, paper no. 51313-02345-SG (Houston, TX: NACE International, 2013).
11. P. Wilson, "Corrosion of Carbon Steel in CO_2 Capture Plant using MDEA and Amino Acid Based Solvents," CORROSION/2012, paper no. 51312-01554-SG (Houston, TX: NACE, 2012).
12. P.C. Rooney, T.R. Bacon, M.S. DuPart, *Hydrocarbon Processing* 75, 3 (1996): p. 95-103.
13. P.C. Rooney, M.S. DuPart, T.R. Bacon, *Hydrocarbon Processing* 76, 4 (1997): p. 65-71.
14. R. Eustaquio-Rincon, M. Esther Rebolledo-Libreros, A. Trejo, R. Molnar, *Ind. Eng. Chem. Res.* 47, 14 (2008): p. 4726-4735.
15. X.P. Guo, Y. Tomoe, *Corros. Sci.* 41, 7 (1999): p. 1391-1402.
16. J. Kittel, R. Idem, D. Gelowitz, P. Tontiwachwuthikul, G. Parrain, A. Bonneau, *Energy Procedia* 1, 1 (2009): p. 791-797.
17. W. Yan, J. Deng, X. Li, X. Dong, C. Zhang, *Chinese Science Bulletin* 57, 8 (2012): p. 927-934.
18. Z.F. Yin, Y.R. Feng, W.Z. Zhao, Z.Q. Bai, G.F. Lin, *Surf. Interf. Anal.* 41, 6 (2009): p. 517-523.
19. Y. Cai, P. Guo, D. Liu, S. Chen, J. Liu, *Science China Technological Sciences* 53, 9 (2010): p. 2342-2349.
20. L. Zheng, J. Landon, W. Zou, K. Liu, *Ind. Eng. Chem. Res.* 53, 29 (2014): p. 11740-11746.
21. M.J. Litchewski, "More Experiences With Corrosion and Fouling in Refinery Amine Systems," CORROSION/96, paper no. 391 (Houston, TX: NACE, 1996).
22. H. J. Liu, J. W. Dean, "Neutralization Technology to Reduce Corrosion from Heat-Stable Amine Salts," CORROSION/95, paper no. 572 (Houston, TX: NACE, 1995).
23. P.C. Rooney, T.R. Bacon, M.S. DuPart, "Effect of Heat Stable Salts on Solution Corrosivity of MDEA-Based Alkanolamine Plants III," 47th Laurance Reid Gas Conditioning Conf. (Norman, OK: University of Oklahoma, 1997).
24. J.G. Green, "Identification of Corrosive Agent in an Industrial Process: Mass Spectrometry as a Part of a Multi-Technique Problem Solving Effort," 39th ASMS Conf. on Mass Spectrometry and Allied Topics (Nashville, TN: ASMS, 1991).
25. S.F. Bosen, S.A. Bedell, "The Relevance of Bicine in the Corrosion of Amine Gas Treating Plants," CORROSION/2004, paper no. 04471 (Houston, TX: NACE, 2004).
26. A.E. Martell, R.M. Smith, "Critically Selected Stability Constants of Metal Complexes," NIST Standard Reference Database no. 46 (Gaithersburg, MD: NIST, 2001).
27. B.B. Benson, D. Krause, Jr., M.A. Peterson, *J. Soln. Chem.* 8, 9 (1979): p. 655-690.
28. P.C. Rooney, D.D. Daniels, *Petroleum Technology Quarterly* 3, 1 (1998): p. 97.
29. J.L. Mora-Mendoza, S. Turgoose, *Corros. Sci.* 44, 6 (2002): p. 1223-1246.
30. R.D. Braun, *Talanta* 38, 2 (1991): p. 205-211.
31. J. Greenberg, M. Tomson, *Appl. Geochem.* 7, 2 (1992): p. 185-190.
32. W. Sun, S. Nešić, R.C. Woollam, *Corros. Sci.* 51, 6 (2009): p. 1273-1276.
33. C.R. Silva, X. Liu, F.J. Millero, *J. Soln. Chem.* 31, 2 (2002): p. 97-108.
34. N. Kladkaew, R. Idem, P. Tontiwachwuthikul, C. Saiwan, *Ind. Eng. Chem. Res.* 48, 19 (2009): p. 8913-8919.
35. N. Kladkaew, R. Idem, P. Tontiwachwuthikul, C. Saiwan, *Ind. Eng. Chem. Res.* 48, 23 (2009): p. 10169-10179.
36. I.R. Soosaiprakasam, A. Veawab, *Int. J. Greenhouse Gas Control* 2, 4 (2008): p. 553-562.
37. G.L. Lawson, A.L. Cummings, S. Mecum, "Amine Plant Corrosion Reduced by Removal of Bicine," Gas Processors Association Annual Convention (San Antonio, Texas: GPA, 2003).